

## Direct observation of laser level occupation and injector coupling in undoped GaAs/(Al,Ga)As quantum-cascade structures

L. Schrottke,<sup>a)</sup> R. Hey, and H. T. Grahn

*Paul-Drude-Institut für Festkörperelektronik, Hausvogteiplatz 5-7, 10117 Berlin, Germany*

(Received 1 December 2003; accepted 6 April 2004; published online 14 May 2004)

The occupation of the laser levels in an undoped GaAs/(Al,Ga)As quantum-cascade structure is directly detected by interband photoluminescence spectroscopy. The upper laser level and the injector state exhibit an anticrossing behavior with a splitting of about 10 meV, which is attributed to a strong coupling between them. The energy splitting matches well the oscillation period observed in recent, ultrafast, coherent electron-transport experiments by F. Eickemeyer *et al.* [Phys. Rev. Lett. **89**, 047402 (2002)]. A comparison with the calculated transition energies qualitatively confirms the anticrossing behavior in the vicinity of the threshold field strength. Furthermore, the measured energy difference between the upper and lower laser level agrees with the lasing energies of a set of complete quantum-cascade lasers. At the same time, the variation of the lasing energies corresponds to the energy splitting between the upper laser level and the injector state. © 2004 American Institute of Physics. [DOI: 10.1063/1.1758774]

Quantum-cascade lasers (QCLs) have attracted much interest for the past decade due to their wide energy range covering the mid- to far-infrared region including the THz regime. The various wavelengths are realized by band structure engineering of semiconductor heterostructures using only a few materials systems.<sup>1,2</sup> The laser transition occurs between subbands within the same (conduction or valence) band. In order to achieve population inversion, a fast carrier transport into the upper laser level is necessary. Usually, QCLs are designed so that an injector couples resonantly with the upper laser level through the so-called injection barrier. Therefore, the population of the upper laser level can be described on the basis of resonant tunneling,<sup>3</sup> which can lead to negative differential resistance effects<sup>4</sup> as well as to an anticrossing behavior of the respective subbands. An independent experimental observation of the anticrossing behavior connected with the occupation of the laser levels would confirm the importance of the tunneling processes for the operation of QCLs.

The strong coupling of the injector state with the upper laser level through the injection barrier leads to a superposition of a bonding and an antibonding state resulting in pronounced gain oscillations. A direct observation of the coherent electron transport properties in QCL structures has been recently reported,<sup>5</sup> where ultrafast quantum transport was investigated by femtosecond midinfrared pump-probe experiments. The oscillation period  $T$  was about 400 fs, which corresponds to an energy splitting  $\Delta E = h/T$  of about 10 meV. In Fig. 1, the envelope functions of the injector state as well as the upper and lower laser level are shown for such a QCL structure. In an earlier study,<sup>6</sup> the influence of the coupling strength on laser operation was investigated by a systematic variation of the thickness of the injection barrier. With decreasing barrier thickness, the intersubband electroluminescence spectra showed a large increase in the line

width.<sup>6</sup> Therefore, an independent determination of coupling of the injector state with the upper laser level would provide valuable information about the transport processes in QCLs.

A rather large splitting of the upper laser level is also expected to broaden the gain spectra. This mechanism could explain the surprisingly large variation of lasing energies of QCLs with nominally identical layer structures of 20 meV, which was observed in a systematic study of the lasing properties of QCLs with different doping concentrations.<sup>7</sup> It cannot be explained by the typical deviations of the layer thickness from the nominal values or by electric-field inhomogeneities due to the carrier distribution. Calculations show that both effects would lead to energy variations of only a few meV.

In this letter, we present an independent analysis of the laser levels and their populations using interband photoluminescence (PL) spectroscopy. In order to avoid line broadening due to electron-electron interactions and heating, we investigated a nominally undoped quantum-cascade structure, i.e., a structure with significantly reduced carrier concentration compared to complete QCLs. The PL spectra allow us to determine the energy positions of both, the upper and the lower laser levels, the splitting between the upper laser level and the injector state, and the population of the subbands.

Quantum-cascade structures are unipolar systems as only electrons (holes) in the conduction (valence) band emit light by intersubband transitions. For the investigation of, e.g., the electron distribution in the conduction band, bipolar interband PL spectroscopy is a powerful tool using photoexcited holes as a probe. However for this case, the hole distribution has to be known. A quantitative study of the electron subband population and the hole dynamics in asymmetric double-quantum-well superlattices<sup>8</sup> led to the conclusion that, for QCL structures with typical barrier thicknesses of 2–3 nm, the majority of photoexcited holes relax very quickly into the widest quantum well (QW) of the active region.<sup>9</sup> As discussed in Ref. 10, heavy holes in the ground valence subband in this QW have a sufficient overlap with

<sup>a)</sup>Electronic mail: lutz@pdi-berlin.de

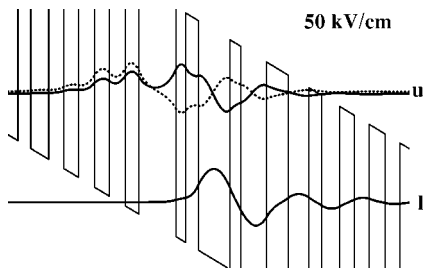


FIG. 1. Calculated envelope functions for the bonding and antibonding states of the coupled injector and upper laser levels ( $u$ , solid and dashed line, respectively) and the lower laser level ( $l$ ) at the critical field strength  $F_{\text{crit}} = 50$  kV/cm. The calculated energy separation between the bonding and antibonding states is about 3 meV.

electrons in the three conduction subbands of the active region. Therefore, a PL signal from all three levels, namely the upper and the lower laser level as well as the lowest subband, is expected as soon as there is a significant subband population by electrons injected from the contacts. Unfortunately, the overlap of the upper laser level with the ground valence band in the widest QW is much smaller than for the lower laser level so that a high excitation power (we used about 40 mW) as well as a sufficient stray light suppression is necessary. This high excitation power is expected to modify the electron distribution. Therefore, we used the anti-Stokes configuration, in which the excitation energy  $E_{\text{exc}}$  is tuned to 1.55 eV, so that carriers are only excited in the contact regions. Note that any PL signal requires electron as well as hole transport into the active region of the QCL structure. The large effective barrier for the holes between the widest QW and the injector leads to a maximum hole concentration in the widest well.

We used a GaAs/(Al,Ga)As QCL structure based on the layer sequence of the original design by Sirtori *et al.*<sup>11</sup> Our sample consists of 20 periods with undoped injectors. The

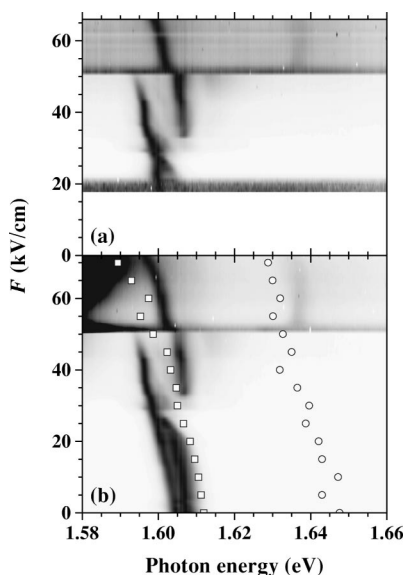


FIG. 2. Normalized, electric-field-dependent PL spectra of the conduction band ground state and the lower laser level below as well as above the critical field strength for both, (a) the anti-Stokes and (b) the Stokes configuration, in a gray-scale representation. For comparison, the calculated transition energies are added (symbols). The splitting of the PL line of the ground state for  $30$  kV/cm  $< F < 50$  kV/cm is probably due to a coexistence of excitons and free electron-hole pairs.

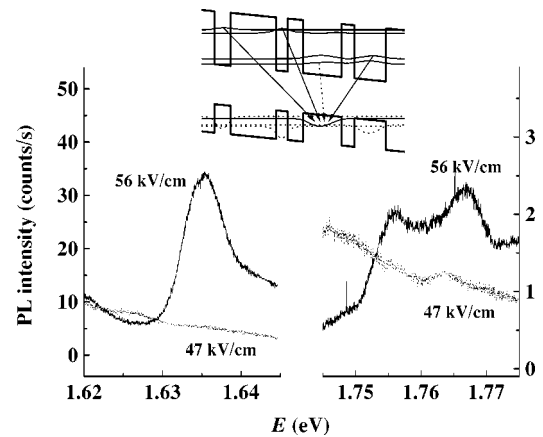


FIG. 3. PL spectra of the lower (left) and upper (right) laser levels below (47 kV/cm) and above (56 kV/cm) the critical field strength. The inset presents a schematic view of the interband PL transitions relevant for QCLs at the operation field strengths.

cladding layers are replaced by simple, 400-nm-thick  $n^+$ -GaAs contact layers in order to eliminate unintentional effects caused by the cladding layers. For comparison, we use a series of complete QCLs with identical layer thicknesses, but different doping densities in the injector.<sup>7</sup> The samples have been grown on  $n^+$ -GaAs(100) substrates by molecular-beam epitaxy. The structures have been characterized by double-crystal x-ray diffraction measurements to demonstrate that the actual layer thicknesses as well as the Al-content fall within 2% of the nominal values. For the optical experiments, the samples were processed into mesa structures with a diameter of about 200  $\mu\text{m}$ , mounted on a cold finger in a He-flow cryostat, and cooled to 5 K. The optical excitation for the PL measurements was carried out by a  $\text{Kr}^+$  laser at a wavelength of 799.3 nm (1.55 eV). For sufficient stray light suppression, the PL emission signal is dispersed in a triple monochromator and detected by a charge-coupled-device camera.

The PL spectra were recorded as a function of the electric field strength  $F$  in the wavelength range for both the lower and upper laser level. First, the electric-field-dependent spectra for the conduction band ground state and the lower laser level have been measured in both the Stokes case ( $E_{\text{exc}} = 1.70$  eV, i.e., excitation above the lower laser

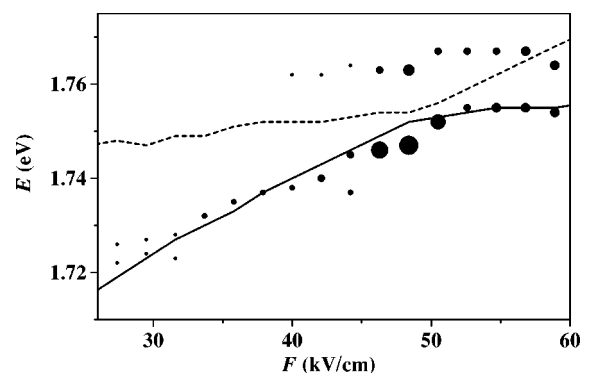


FIG. 4. Transition energies for the upper laser level and the injector state for recombination into the valence ground state as a function of electric field strength (symbols). The size of the symbols approximately represents the intensity normalized by the intensity of the ground-state transition at about 1.60 eV. For comparison, the calculated values are added (lines).

level, but below the barrier) and the anti-Stokes case. As shown in Fig. 2 for weak excitation power, the two experiments lead to the same results, i.e., for both cases, the vast majority of photoexcited holes are trapped in the ground state of the widest well. Any influence of a variation in the hole densities for different periods on the PL spectra can be neglected. Figure 3 shows the PL spectra of the lower and upper laser levels for  $F=47$  kV/cm (below a critical field strength  $F_{\text{crit}}=50$  kV/cm) and  $F=56$  kV/cm (above  $F_{\text{crit}}$ ). While below  $F_{\text{crit}}$ , almost no signal is detected from the lower or from the upper laser level, clear evidence of their population is obtained for the higher field strength. The population ratio  $\rho_n = n_u/n_l$ , where  $n_u$  ( $n_l$ ) denotes the occupation of the upper (lower) laser level, is estimated from  $\rho_n = \rho_I/\rho_M$ . Here  $\rho_I = I_u/I_l$  refers to the ratio of the integrated PL intensities  $I_u$  and  $I_l$  and  $\rho_M = M_u/M_l$  to the ratio of the transition matrix elements  $M_u$  and  $M_l$  of the upper and lower laser levels, respectively. From the experiments, we obtain  $\rho_I \approx 0.02$ , while the ratio of the overlap integrals of the calculated envelope functions leads to  $\rho_M \approx 0.01$ . The resulting value of about 2 is fairly constant for field strengths between 50 and 60 kV/cm. This observation confirms the idea that the population ratio depends mainly on the lifetimes of the states.

The PL line attributed to the upper laser level is clearly split into two. The energy separation between the two peaks of the upper laser level and the lower laser level is 120 and 132 meV so that  $\Delta E = 12$  meV. Since the total line width (20 meV) is larger than  $\Delta E$ , this result agrees very well with the range of lasing energies (115–135 meV) as reported in Ref. 7. Therefore, we believe that the splitting broadens the gain spectrum. The mechanism, which is responsible for the large variation of the lasing energies of nominally identical lasers, is probably based on the interplay of the broad gain curve with a likewise broad loss spectrum. Small changes of the loss spectrum due to different properties of the resonator or different carrier concentrations are expected to lead to the observed broad range of lasing energies.

In order to verify that the splitting of the PL line attributed to the upper laser level is due to the coupling of injector and laser level, we have plotted the energies of the two peaks as a function of the electric-field strength in Fig. 4. As expected, an anticrossing-like behavior is observed. For comparison, we added the calculated transition energies of the upper laser level and the injector state with the valence-band ground state. For the calculation, we solved the Schrödinger equation in the envelope function approximation with an effective mass linearly dependent on energy in order to take into account nonparabolicity effects. The nonparabolicity parameter is tuned so that the calculated critical field strength defined by the anticrossing agrees with the experimentally determined one.

For the lower-energy branch of the two coupled states, the calculated transition energies agree very well with the experimental values. However, for the higher-energy branch, the measured energy values are much larger than the calculated ones, i.e., the splitting energy is larger than expected. This discrepancy can only partially be overcome by adjusting the materials parameters, e.g., a decrease of the barrier

height by 20 meV would increase the splitting from about 3 to about 5 meV.

Comparison with the current–voltage characteristics shows that a current instability occurs at  $F_{\text{crit}}$ ,<sup>10</sup> which indicates a rather high density for the injected carriers at this field strength even in the case of undoped quantum-cascade structures. Furthermore, there is a redshift at higher field strengths in particular for the higher-energy branch, which may be caused by field inhomogeneities due to the increased carrier density. Therefore, we believe, that an improvement of the calculations can be achieved when the spatial carrier distribution is taken into account by a self-consistent solution of the Schrödinger and Poisson equations. However, the total carrier density has to be determined independently. It is assumed to increase with increasing applied voltage due to an electric-field-dependent injection efficiency of the contacts.

Despite the deviation of the calculated energies of the upper branch from their experimental values, the measured energy separation  $\Delta E = 12$  meV agrees well with the value of 10 meV estimated from the oscillation period in the ultrafast quantum transport experiment described in Ref. 5. Therefore, we conclude that the splitting (and hence in part the broad gain curve) is caused by the coupling of the injector with the upper laser level. However, the coupling between these two quantum levels seems to be stronger than expected from the simple envelope function calculation.

In conclusion, we have observed the upper and lower laser levels of a QCL and their population by electric-field-dependent interband PL spectroscopy. The difference in the measured transition energies agrees very well with the lasing energies of corresponding QCLs.<sup>7</sup> The observed splitting between the upper laser level and the injector level agrees with results of quantum transport experiments,<sup>5</sup> but is larger than the calculated value.

The authors are grateful to M. Ramsteiner for assistance with PL measurements and M. Giehler for helpful discussions. This work was supported in part by the Deutsche Forschungsgemeinschaft within the framework of the Forschergruppe 394.

<sup>1</sup>J. Faist, F. Capasso, D. L. Sivco, C. Sirtori, A. L. Hutchinson, and A. Y. Cho, *Science* **264**, 553 (1994).

<sup>2</sup>C. Gmachl, F. Capasso, D. L. Sivco, and A. Cho, *Rep. Prog. Phys.* **64**, 1533 (2001), and references therein.

<sup>3</sup>C. Sirtori, F. Capasso, J. Faist, A. L. Hutchinson, D. L. Sivco, and A. Y. Cho, *IEEE J. Quantum Electron.* **34**, 1722 (1998).

<sup>4</sup>C. Sirtori, H. Page, C. Becker, and V. Ortiz, *IEEE J. Quantum Electron.* **38**, 547 (2002).

<sup>5</sup>F. Eickemeyer, K. Reimann, M. Woerner, T. Elsaesser, S. Barbieri, C. Sirtori, G. Strasser, T. Müller, R. Bratschitsch, and K. Unterrainer, *Phys. Rev. Lett.* **89**, 047402 (2002).

<sup>6</sup>S. Barbieri, C. Sirtori, H. Page, M. Stellmacher, and J. Nagle, *Appl. Phys. Lett.* **78**, 282 (2001).

<sup>7</sup>M. Giehler, R. Hey, H. Kostial, S. Cronenberg, T. Ohtsuka, L. Schrottke, and H. T. Grahn, *Appl. Phys. Lett.* **82**, 671 (2003).

<sup>8</sup>L. Schrottke, R. Hey, and H. T. Grahn, *Appl. Phys. Lett.* **79**, 629 (2001).

<sup>9</sup>L. Schrottke, R. Hey, H.-Y. Hao, T. Ohtsuka, and H. T. Grahn, *Physica E (Amsterdam)* **13**, 866 (2002).

<sup>10</sup>L. Schrottke, R. Hey, H. Kostial, T. Ohtsuka, and H. T. Grahn, *Physica E (Amsterdam)* **21**, 852 (2004).

<sup>11</sup>C. Sirtori, P. Kruck, S. Barbieri, P. Collot, J. Nagle, M. Beck, J. Faist, and U. Oesterle, *Appl. Phys. Lett.* **73**, 3486 (1998).